

Emissions and Chemical Components of PM_{2.5} from Simulated Cooking Conditions Using Traditional Cookstoves and Fuels under a Dilution Tunnel System

Colleen Marciel F. Rosales^{1†}, Jinsang Jung², Mylene G. Cayetano^{3,4*}

¹ Institute of Chemistry, University of the Philippines, Diliman, Quezon City 1101, Philippines

² Korea Research Institute of Standards and Science, Daejeon 34113, Korea

³ Institute of Environmental Science and Meteorology, University of the Philippines, Diliman, Quezon City 1101, Philippines

⁴ International Environmental Research Institute, Gwangju Institute of Science and Technology, Gwangju 61005, Korea

ABSTRACT

Despite the considerable cost associated with estimating household emissions from solid fuel, which are frequently undetected by air quality monitoring systems, compiling such an inventory is critical to identifying the link between indoor pollution and health effects. Therefore, this study used the UP Diliman dilution tunnel system (UPDDTS) to characterize the composition of particulate matter in the smoke and quantify the PM_{2.5} emitted by traditional Philippine cooking systems, *viz.*, a charcoal-burning cement stove (CCP), a sawdust-burning tin-can stove (KKP), a fuelwood-burning metal-grill stove (MFP), a kerosene-burning metal stove (MKP), and a charcoal-burning metal-grill stove (MCC). Forty-three sampling tests revealed that water-soluble K⁺ ($23.0 \pm 1.9 \mu\text{g m}^{-3}$), Cl⁻ ($12.3 \pm 1.0 \mu\text{g m}^{-3}$), and Na⁺ ($43 \pm 22 \mu\text{g m}^{-3}$) contributed to the majority of the ionic mass concentrations generated by the CCP and MKP, respectively, whereas levoglucosan—a signature of biomass burning—dominated the PM_{2.5}-bound monosugars emitted by the KKP ($78.72 \pm 6.96 \mu\text{g m}^{-3}$), MFP ($0.76 \pm 0.34 \mu\text{g m}^{-3}$), and MCC ($10.21 \pm 2.64 \mu\text{g m}^{-3}$). The abundance of the water-soluble organic carbon (WSOC) in all of the samples, except those from the MKP, depended on the surface area—and thus the facet—of the fuel. Additionally, the elemental compositions of the PM_{2.5} from the CCP, KKP, and MCC mainly consisted of Pb (1.96 ± 1.04 to $76.02 \pm 151.42 \text{ ng min}^{-1}$), but those for the MFP and KKP primarily contained Cu ($2.23 \pm 1.18 \text{ ng min}^{-1}$) and As ($5.51 \pm 1.08 \text{ ng min}^{-1}$), respectively. The PM_{2.5} emission rates exceeded the World Health Organization (WHO)'s emission rate target guideline for ventilated conditions (0.8 mg min^{-1}) by 1.9×10^6 to $23 \times 10^6 \text{ mg min}^{-1}$, and the highest PM_{2.5} emission factor, $0.032 \pm 0.016 \text{ kg-PM}_{2.5} \text{ kg-fuel}^{-1} \text{ y}^{-1}$, which was exhibited by the MKP, surpassed values in the literature by three orders of magnitude.

Keywords: Emission inventory, Emission factor, dilution tunnel, Particulate matter, Air quality

1 INTRODUCTION

Household energy use remains to be directly linked to health risks, since people have always relied on cookstoves and fuels of varying quality for daily supply of food, while smoke emitted from the use of these cookstoves and fuels can compromise indoor air quality. According to the United Nations Development Programme (UNDP), there are around 3 billion people that still rely on wood, coal, charcoal, or animal waste for cooking and space heating (UN, 2018). This translates to about 4.3 million premature deaths in 2012 globally due to household air pollution from using solid fuels for household energy, with the highest percentage in the low- and middle-income countries (LMICs) (UN, 2018). In the Philippines, traditional cookstoves such as cement stoves and

OPEN ACCESS



Received: November 7, 2020

Revised: January 28, 2021

Accepted: February 25, 2021

* **Corresponding Author:**

mcayetano@iesm.upd.edu.ph

† **Present address:**

O'Neill School of Public and Environmental Affairs, Indiana University, Bloomington, Indiana 47405, USA

Publisher:

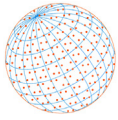
Taiwan Association for Aerosol Research

ISSN: 1680-8584 print

ISSN: 2071-1409 online

© **Copyright:** The Author(s).

This is an open access article distributed under the terms of the [Creative Commons Attribution License \(CC BY 4.0\)](https://creativecommons.org/licenses/by/4.0/), which permits unrestricted use, distribution, and reproduction in any medium, provided the original author and source are cited.



metal grills, both of which use either charcoal or fuelwood, are still ubiquitous. These traditional cookstoves are used for tenderizing meat, low-cost cooking (usually by the underprivileged sector who cannot afford cleaner cookstoves), small-scale income generation, meat-grilling, or simply cooking daily household food. Small-scale smoke houses are rampant in the cities and are unregulated. It is estimated, based on white papers, that around 57% of the population rely on traditional solid fuels (charcoal and fuelwood) for cooking and heating (PSA, 2014). With a population of 100.98 million (PSA, 2015) and rising, the usage of these traditional cookstoves and solid fuels provide required energy for a significant percentage of households. However, inefficient cookstoves and traditional fuel burnings result in a range of health impacts. For example, 84 deaths per 100,000 persons in the Philippines are attributable to these indoor air pollutants (WHO, 2016; Yee, 2018). Moreover, it was found to disproportionately affect the low- and middle-income households (Gloor, 2014). Pertinent diseases include the incidence of acute lower respiratory infections (ALRIs) and chronic obstructive pulmonary disease (COPD). A few studies that focused on household exposures from cooking in low-income countries have been conducted in the past, such as one by Saksena *et al.* (2007) where 120 houses were subjected to a socioeconomic survey and 30 houses were sampled for carbon monoxide and particulate matter (PM). With an estimate of over half of Filipinos being exposed to these household indoor cooking pollutants and a relative lack of information on their long-term exposure effects, the challenge of household air pollution issues remains to be tackled. Furthermore, there is a need to create such awareness for the general public and policy makers.

In order to estimate emissions from household energy use, measurements may be performed in each individual household through surveys (GIZ, 2012)—as in Saksena *et al.* (2007)—and individual testing (Aguilar *et al.*, 2017). However, these may be costly and time-consuming. Simulating cooking activities under a dilution tunnel is becoming more popular (Jenkins, 1990; Rapp, 2017) and cooking activity data may be obtained by gathering observational or secondary data from entities that hold information about fuel use or other proxy measurements, such as number of households or small businesses that still utilize traditional cookstoves and fuels. In addition, databases such as EMEP/EEA (European Monitoring and Evaluation Programme/European Environment Agency) CORINAIR, an inventory of emissions of air pollutants in Europe (European Environment Agency, 2009) or U.S. Environmental Protection Agency's AP-42 (U.S. EPA, 2009) may not be reflective of LMIC emissions. Thus, resulting emission factors from dilution tunnels are useful and practical tools for carrying out emissions inventories and modeling products that may be more relevant to policy makers and environmental health managers in local settings.

In this study, a testing chamber (dilution tunnel) was utilized to simulate cooking activities using four different cookstoves and varying three commonly used fuels. The smoke generated was collected for PM_{2.5}. Filter substrates were analyzed for particulate mass, ions, monosugars, carbon, and elemental composition. The relationship among the chemical components with respect to the fuel burned were analyzed using Statgraphics Centurion XVII. The results from the elemental and chemical analyses were used to (a) calculate PM_{2.5} emission factors ($\text{kg-PM}_{2.5} \text{ kg-fuel}^{-1} \text{ y}^{-1}$), (b) calculate elemental emission factors for As, Cd, Co, Cu, Mn, Ni, Pb, and Sr, and (c) assess chemical fingerprints using ion concentrations (Li^+ , Na^+ , NH_4^+ , K^+ , Mg^{2+} , Ca^{2+} , Cl^- , SO_4^{2-} , and NO_3^-), monosugar levels (levoglucosan, mannosan, and galactosan), and water-soluble organic composition. Lastly, the emission rates of the cookstoves and fuels were determined and compared with World Health Organization emission rates for cookstoves and fuels under vented conditions.

2 METHODS

2.1 Selection and Testing of Cookstoves and Fuels

The traditional cookstoves and fuels tested were those commonly used in the Philippines (Fig. 1): (1) CCP—cement cookstove in charcoal, (2) KKP—*kasong* (tin can) cookstove in *kusot* (saw dust) from red lauan tree (*Shorea negrosensis*), (3) MFP—metal-grill cookstove in fuelwood (mango tree, possibly *Mangifera indica*), and (4) MKP—metal cookstove in kerosene. The cooking substrate—metal frying pan—was conducted in this particular set of tests, as the test activities were conducted before the Harmonized Laboratory Test Protocol TC 285 (including Water Boiling Test 4.2.3 Protocol by the Global Alliance for Clean Cookstoves) was published in 2018 (CCA, 2018). In addition, a metal-grill cookstove in charcoal (MCC) was also tested while simulating

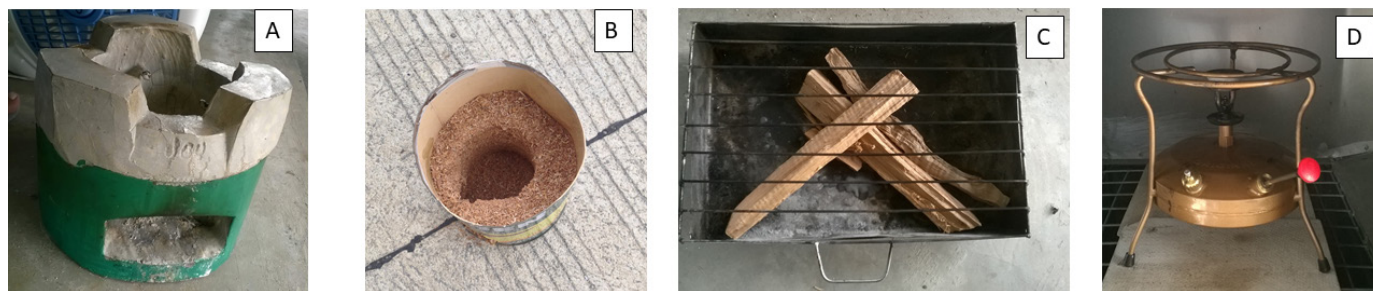
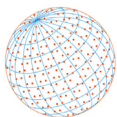


Fig. 1. Traditional cookstoves and fuels tested: (A) CCP, (B) KKP, (C) MFP (same grill was used for MCC), and (D) MKP.

Table 1. Sampling code, cooking simulations, and duration for the tested cookstoves and fuels.

Code	Cookstove and fuel	Cooking simulation	Test duration	<i>N</i>
CCP	Cement and charcoal	Pan-frying in oil	60	9
KKP	<i>Kasong</i> (tin can) and <i>kusot</i> (saw dust)	Pan-frying in oil	60	8
MFP	Metal-grill and fuelwood	Pan-frying in oil	30–40	9
MKP	Metal and kerosene	Pan-frying in oil	30	9
MCC	Metal-grill and charcoal	Chicken grilling	80	8

chicken grilling (*lechon manok*), to represent the ubiquitous small-scale commercial rotisseries in Philippine cities. The cooking simulations lasted for 30–80 minutes (Table 1).

At least eight sampling trials and one background run were performed for each test material. For each sample, the following parameters were recorded: filter code (associated with a pre-weight), sampling description, trial start and end times, blower fan setting, cleaning start and end times, weight and/or volume of test material or fuel before and after burning, wind speed, and temperature at four different points in the test chamber. For MFP and KKP, a small amount of kerosene was added to initiate the burning process. Since this amount is small and insignificant with respect to the amount of fuelwood and sawdust burned, it was not included in the calculation of the emission rates.

2.2 Design and Fabrication of the Dilution Tunnel

The UP Diliman dilution tunnel system (UPDDTS) used for testing the traditional cookstoves and fuels (Fig. 2) was based on the concept of Jenkins (Jenkins, 1990), and satisfies the requirements of: (1) an enclosed system with a variable speed blower to mix ambient air with cookstove emission before sampling, (2) a test chamber where the stoves are tested and fuel burned, (3) a sampling chamber for the collection of smoke samples, and (4) an exhaust system to minimize emissions to the atmosphere. It has a square cross section and a hydraulic diameter of 0.5 meter.

At the beginning of a sampling day, the UPDDTS was cleaned with diluted detergent, rinsed, and then air dried by turning the electric fan (variable speed blower) on for at least 15 minutes. Temperature and wind velocity were measured at four different points (blower section, test chamber, sampling chamber, and exhaust outlet) using a portable handheld anemometer (generic handheld anemometer and thermometer; LatestGadget.com.ph Online Store). The average wind velocity in each section are reported in Table 2, and range from 2–4 m s⁻¹. Average wind velocities in each section remained the same during the background and the testing except in the sampling chamber itself, where the temperature change may have been greatest. The average temperature in the test chamber is about 36°C; the average temperatures in the other points are 32°C (blower), 34°C (sampling chamber), and 33°C (exhaust pipe outlet).

2.3 Sampling PM_{2.5} from Cookstoves and Fuel in a Simulated Cooking Condition

PM_{2.5} were collected on pre-conditioned polytetrafluoroethylene (PTFE) substrates (0.45 μm pore size, 47 mm diameter; Whatman®). The PTFE substrates were subjected to static removal pre- and post-weighing in a microbalance (ME5-F; Sartorius). The filter substrates were used to collect the emissions from the test materials using a mini-volume sampler (MiniVol; Airmetrics)

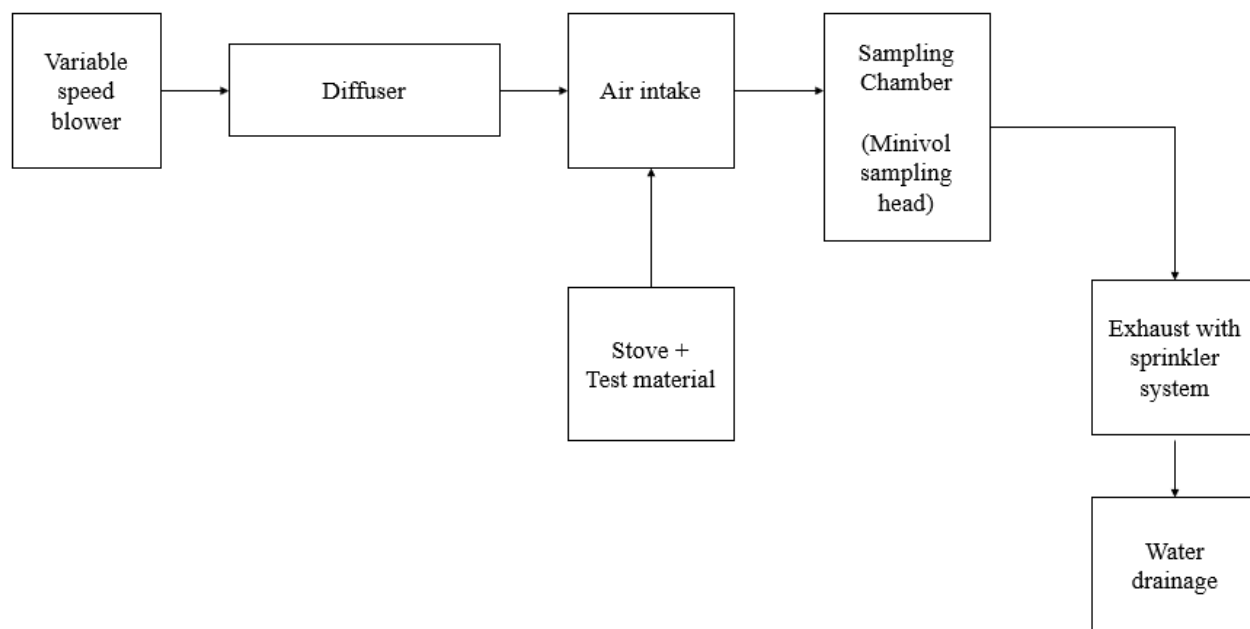
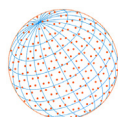


Fig. 2. Design of the UPD dilution tunnel system (UPDDTS).

Table 2. Performance conditions of the UPDDTS.

Measurement point	Background ($N = 12$)		Testing ($N = 40$)		Remarks ^a
	Wind velocity, m s^{-1}	$Re (\times 10^5)$	Wind velocity, m s^{-1}	$Re (\times 10^5)$	
Blower section	4 ± 1	1.4 ± 0.4	4 ± 1	1.3 ± 0.4	Turbulent
Test chamber	3 ± 1	0.9 ± 0.4	3 ± 1	0.8 ± 0.3	Turbulent
Sampling chamber	3 ± 2	0.9 ± 0.6	4 ± 2	1.2 ± 0.8	Turbulent
Exhaust outlet	2 ± 1	0.7 ± 0.4	2 ± 1	0.8 ± 0.4	Turbulent

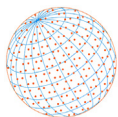
^a The flow is turbulent if the $Re > 4 \times 10^3$.

at a flow rate of 5 L min^{-1} with a $\text{PM}_{2.5}$ size cut impactor. The filters were portioned in half and each half was weighed using a microbalance (Cahn C-33; Thermo).

2.4 Elemental Analysis of Filters

One half of each filter was analyzed for elemental composition using inductively coupled plasma mass spectrometry (ICP-MS; 7500 Series; Agilent Technologies). The sample was prepared for analysis by digestion in hot acid (closed-vessel microwave digester; ETHOS One) (Kulkarni *et al.*, 2007). The rings of the PTFE half-filters were removed prior to digestion to allow for all heat to be directed to the PM bound to the filter. The half-filter was digested using 18.5% HNO_3 . This concentration was chosen so that the final acid concentration after dilution is within 4% to avoid corrosion of the ICP-MS cones (Kulkarni *et al.*, 2007). The digestion method employed 20 minutes of ramping up to 200°C , 10 minutes of holding at this temperature, 10 minutes of cooling down the vessel inside the digester, and 20 minutes of cooling down the vessel outside the digester. The maximum energy input was 1000 W.

A multi-elemental ICP-MS calibration standard ($10 \mu\text{g mL}^{-1}$ in 5% HNO_3 + tr HF; Peak Performance certified reference materials) was used for external calibration of 14 elements (Al, As, Ca, Co, Cd, Cr, Cu, Mg, Mn, Na, Ni, Pb, Sr, and Zn). Standard concentrations used were 0, 0.01, 0.05, 0.1, 0.5, 1, 5, 10, 50, 100, and 500 ppb. Calibration curves were generated using the ICP-MS software and concentrations of the elements in the sample digestates were calculated in this program. Individual blank PTFE filters were spiked with known amounts of the elements (0.1, 0.2, 0.25, 0.5, 0.75, and 1 mL of 10 ppm multi-elemental standard) and digested with the same method used for the samples to conduct recovery tests.



2.5 Analysis of Water-soluble Ions, Organic Carbon, and Cellulose Degradation Products

Ultrapure water used in this study was prepared using a Labpure S1 filter with a UV lamp, with resistivity and total organic carbon (TOC) values of $18.2 \text{ M}\Omega \text{ cm}^{-1}$ and 1 ppb, respectively (PURELAB Ultra; ELGA). A quarter of the filter was extracted with 12 mL organic-free ultrapure water under ultrasonication for 30 minutes. Extracted samples were then filtered through a $0.45 \mu\text{m}$ syringe filter (Acrodisc®; Pall Gelman) to remove water-insoluble suspended materials. Filtered water extracts were stored in a refrigerator at 4°C until analysis. An aliquot (1.2 mL) of the water extract was used in the analysis of cations and anions using ion chromatography (Dionex ICS-5000; Thermo Fisher Scientific). Cations which include sodium [Na^+], potassium [K^+], ammonium [NH_4^+], calcium [Ca^{2+}], and magnesium [Mg^{2+}] were separated using CS-12A column at a flow rate of 1 mL min^{-1} . For the anions, sulfate [SO_4^{2-}], nitrate [NO_3^-], and chloride [Cl^-] were separated using AS-15 column at 1.2 mL min^{-1} flow rate. Measurement calibrations for cations and anions were performed using Dionex Six Cation Standard II and Seven Anion Standard, respectively. Cation and anion standard concentrations used in the analysis were 0.2, 0.5, 1.0, and 2.0 ppm. Standards were measured before and after each analytical sequence. Eight spiked samples were also analyzed prior to test samples to validate method and instrument performance. A spiked sample was also analyzed for every batch of 10 samples.

To measure water-soluble organic carbon (WSOC), a quarter of the filter was extracted with 20 mL ultrapure water in a glass vial using an ultrasonic extractor for 30 minutes. The water extracts were filtered with a syringe filter ($0.4 \mu\text{m}$ PTFE membrane; Pall Corp.) and then introduced to a total organic carbon analyzer (TOC-LCSH/CSN; Shimadzu). In the TOC analyzer, the water extract was acidified using HCl and then bubbled with pure N_2 gas to eliminate the inorganic carbon component. Then, the organic compounds in the water extracts were combusted at 680°C with a platinum catalyst to form CO_2 , which was then quantified using a nondispersive infrared (NDIR) sensor. The instrument was calibrated with known amounts of potassium hydrogen phthalates [$\text{C}_6\text{H}_4(\text{COOK})\text{COOH}$] solution.

Levoglucosan was analyzed by an improved high-performance anion exchange chromatography (HPAEC) method with pulsed amperometric detection (PAD) (Engling *et al.*, 2006; Jung *et al.*, 2014). The HPAEC-PAD system uses an ion chromatograph consisting of an electrochemical detector and gold electrode unit, along with an AS40 Autosampler (Dionex ICS-5000; Thermo Fisher Scientific). Levoglucosan was separated by a CarboPac MA1 analytical column ($4 \times 250 \text{ mm}$) and a sodium hydroxide solution as eluent. The detection limit of levoglucosan was 3.0 ng m^{-3} . The analytical error, defined as the ratio of the standard deviation to the average value and obtained from triplicate analyses of filter samples, was 1.9%.

3 CALCULATIONS

3.1 Performance of the UPDDTS

The following equation was used to calculate the Reynolds number (Re) of the UPDDTS, an indicator of the flow regime of the testing chamber:

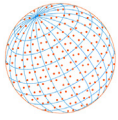
$$Re(\text{unitless}) = \frac{\rho \times u \times L}{\nu} \quad (1)$$

where ρ is the density of dry air at 1.0 atm and 20°C (kg m^{-3}), u is the velocity (m s^{-1}), L is the hydraulic diameter (m), and ν is the viscosity of dry air ($\text{kg m}^{-1} \text{ s}^{-1}$) (Engineering ToolBox, 2003).

The air exchange rate per hour under the UPDDTS test section was calculated using the general formula for air change per hour (ACH):

$$ACH(\text{h}^{-1}) = \frac{Q \times 60}{\text{Area} \times \text{height}} \quad (2)$$

where Q is the volumetric flow rate ($\text{m}^3 \text{ s}^{-1}$) of the air flow inside the UPDDTS (in this case, the



average velocity (m s^{-1}) multiplied by the UPDDTS cross-sectional area (m^2), and 60 is a conversion factor from seconds to hours. The ACH is then used to calculate the $\text{PM}_{2.5}$ emission rates of each stove and fuel combination tested.

3.2 Quality Assurance in Chemical Analysis

Concentrations of the elements were reported in ppb (as calculated by the ICP-MS software), and in ng m^{-3} , which was calculated using the formula:

$$\text{conc (ngm}^{-3}\text{)} = \text{conc ppb (ngL}^{-1}\text{)} \times \frac{\text{volume of solution, L}}{\text{volume of air sampled in filter, m}^3} \quad (3)$$

where the volume of solution is 0.050 L, and the volume of air sampled, in m^3 , is calculated using Eq. (3.1):

$$\begin{aligned} & \text{volume of air sampled (m}^3\text{)} \\ &= \text{flow rate of MiniVvol} \times \text{length of sampling} \times \text{conversion factor} \\ &= 5 \frac{\text{L}}{\text{min}} \times (0.5 \text{ to } 1.3) \text{ hr} \times 60 \frac{\text{min}}{\text{hr}} \times \frac{0.001 \text{ m}^3}{1 \text{ L}} \end{aligned} \quad (3.1)$$

Detailed methodology for the method validation for this analysis and MDL values in ppb are reported in Rosales and Lamorena-Lim (2015). Briefly, recovery was calculated using Eq. (4):

$$\% \text{ recovery} = \frac{(C_s - C)}{S} \times 100 \quad (4)$$

where C_s is the measured concentration of the spiked sample, C is the measured concentration of the unspiked sample (background concentration), and S is the theoretical concentration of the spiked sample. Method detection limit (MDL) was calculated using Eq. (5):

$$\text{MDL} = t \times S \quad (5)$$

where t is the Student's t -value at 99% confidence level ($t_7 = 3.14$), and S is the standard deviation of the seven spiked replicates.

3.3 Emission Rates and Emission Factors

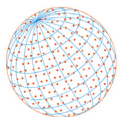
The $\text{PM}_{2.5}$ emission rates were calculated using Eq. (6):

$$\text{Emission rates} = \frac{(\text{mass concentration of } \text{PM}_{2.5} \text{ on filter, } \mu\text{g m}^{-3}) \times \text{duration of cooking}}{\text{ACH}} \quad (6)$$

The emission factors were calculated as:

$$\begin{aligned} & \text{Emission factor} \\ &= \frac{\text{mass of } \text{PM}_{2.5} \text{ or element on filter, kg}}{(\text{mass or volume of fuel burned, kg or L}) \times (\text{average burning time in a year})} \end{aligned} \quad (7)$$

For solid fuels, the denominator is mass (kg), while for liquid fuel (kerosene), it is in volume (L). Corrections were calculated as necessary, incorporating the method blanks and emission factor of kerosene (if added). Largest uncertainties in calculations arise from (1) the mass or volume of material used, because of the uncertainties in measurements of material mass before and after burning, and (2) the average burning time in a year, which was estimated from activity data.



3.4 Correlation Analysis

Pearson correlation coefficients, which measure the strength of a linear relationship between the variables, were calculated using Statgraphics Centurion XVII. Analyses were performed at 95.0% confidence level. *p*-values were calculated to evaluate the statistical significance of the estimated correlations.

4 RESULTS AND DISCUSSION

4.1 Performance of the UPDDTS

In testing cookstoves, it is important that the emissions be well mixed and unbiased at the point of sampling (sampling chamber) so that the PM_{2.5} sampler can take representative samples of the smoke (Wilson *et al.*, 2017). Thus, it is important that there is turbulent mixing within the UPDDTS. From the UPDDTS data, wind velocity and *Re* at various measurement points are shown in Table 2, satisfying turbulent flow within the tunnel system.

In the UPDDTS, the distance between the test chamber and the sampling chamber is 2 meters (79" or ~8 duct diameters), at a flow rate of 2700 m³ h⁻¹ and *Re* that ranged from 0.8×10^5 to 1.2×10^5 . This performance is an order of magnitude greater than Lawrence Berkeley National Laboratory's dilution tunnel setup at a flow rate of 340 m³ h⁻¹ and *Re* at 3.9×10^4 (Wilson *et al.*, 2017). Although the UPDDTS was not tested for accuracy using pulsed tracer gases, Wilson *et al.* (2017) suggested that a dilution tunnel between 7–10 duct diameters, satisfies turbulent flow and would have well-mixed sampled emissions. However, a turbulent flow will also introduce particle loss to the walls, which was not quantified in this study. This would mean that values presented herein could possibly be lower than actual emissions in an open environment. However, one would expect that losses may not be very significant when the tunnel is at a higher temperature such that no condensation occurs on the walls of the tunnel. Hildemann (1989) reported that for a turbulent dilution tunnel (*Re* = 10,000) with a large diameter, particle loss is only about 1–2%.

4.2 Particulate Emission Rates and Emissions

The extent of impact of emissions from cookstoves and fuels on household air quality are determined by the emission rates. Emission rate targets are established by correlating specific health risks to emissions, and compliance to which may assess how well various interventions can meet the air quality concentrations specified in the WHO guidelines. The WHO provided a PM_{2.5} emission rate target (ERT) of 0.8 mg min⁻¹ for cookstoves used under vented kitchen conditions. If complied with, household air quality would meet the annual final PM_{2.5} guideline value of 10 µg m⁻³ (WHO, 2014). When tested under the performance conditions of the UPDDTS, cookstoves and fuels in this study range from 1.9×10^6 to 23×10^6 mg min⁻¹ (Table 3), several orders of magnitude higher than the WHO ERT at 0.8 mg min⁻¹. Hence, the design of the UPDDTS does not only provide satisfying performance of the mixing of sampled air, but it also can provide a means to determine whether the cooking equipment and fuel can meet the annual air quality guideline value of 10 µg m⁻³ under a vented condition.

Table 3. PM_{2.5} emission rates and emission factors.

Stove + fuel (<i>N</i> = number of trials)	PM _{2.5} emission rate ^a , mg min ⁻¹ ($\times 10^6$)	PM _{2.5} emission factor, kg-PM _{2.5} kg-fuel ⁻¹ y ⁻¹ per average burning time (365-day emission) ^{b,c}	Literature values, kg-PM kg-fuel ⁻¹ y ⁻¹
MCC (<i>N</i> = 8)	7.8 ± 4.0	0.008 ± 0.004	0.100 ^d
CCP (<i>N</i> = 9)	11.0 ± 4.0	0.015 ± 0.005	0.020 ^e
KKP (<i>N</i> = 8)	23.0 ± 4.0	0.019 ± 0.002	–
MFP (<i>N</i> = 9)	1.9 ± 1.4	0.023 ± 0.027	0.014 ^e
MKP (<i>N</i> = 9)	2.8 ± 1.3	0.032 ± 0.016	0.00035 ^e

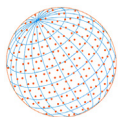
^a WHO emission rate target for PM_{2.5} emission rates for vented facilities: 0.8 mg min⁻¹.

^b kg-PM_{2.5} L-fuel⁻¹ y⁻¹ for kerosene.

^c 12 hours for MCC, 6 hours for the rest.

^d Suranaree University of Technology (STU), 2012.

^e EMEP/EEA, 2009.



Emission factors for PM_{2.5} calculated using Eq. (7) are shown in Table 3. MCC values were compared to the PM emission factor reported in an emissions inventory by the Suranaree University of Technology in 2012, in which the emission factor was obtained by performing street cooking experiments (grilling and barbecuing of chicken and pork) in a burning chamber. This value is much larger than what was obtained using the present setup. However, a direct comparison between the two values may not be appropriate because of the differences in sampling methodologies employed in the burning experiments and the PM reported in literature is total PM (PM_{2.5} up to TSP) (SUT, 2012). In addition, the calculated PM_{2.5} emission rate in this study is only 8% of the literature value for MCC (Table 3), likely due to a smaller PM_{2.5} contribution (less than 1%) to the total particle concentration as compared to larger particle sizes (Baldauf *et al.*, 2016).

For the CCP and MFP, the calculated PM_{2.5} emission factors are in the same order of magnitude and are therefore in reasonable agreement with the EMEP/EEA values. MFP is higher by a factor of two, but CCP is lower than the literature value. The difference in the values in this work is due to the difference in the type of organic matter or wood sampled and thus a straightforward comparison may not be appropriate.

For MKP, the order of magnitude obtained using the UPDDTS is much higher than literature but within the same order of magnitude calculated for the other sources. This is due to the difference in the composition or grades of kerosene produced in the Philippines than those in developed countries. Cleaner technologies allow for cleaner fuels to be produced in developed countries, whereas crude burning of kerosene with simple, low-technology cookstoves allow for emission of more PM, especially PM_{2.5}, and thus make the user more vulnerable to pollutant exposure. This shows that if literature values were used for emission inventories, it may cause underestimations of emissions from kerosene.

Comparison of tested emission sources show that while KKP has the highest emission rate per minute (second column, Table 3), MKP has the highest emission factor based on the amount of fuel used in a year, i.e., kg-PM_{2.5} kg-fuel⁻¹ y⁻¹ per average burning time (third column, Table 3). The high emission rate of KKP as compared to the other sources is caused by introducing very fine, grainy wood shavings, as opposed to fuelwood and charcoal having greater surface areas and therefore would take more time to burn and give off smaller particulates. Thus, the size of the raw material (apart from the weight) can be considered as one of the factors that affect the amount of particulate matter emitted by a certain emission source. However, as for kerosene, the amount of particulate matter emitted is dependent on its density. It should be noted, however, that the filter for kerosene was the blackest, which shows more black carbon (incomplete combustion) as kerosene is purely hydrocarbon. However, these particles might be in the fine-to-ultrafine size range and might therefore be larger in number but lesser in weight as compared to those in the PM_{2.5} cut point collected from the solid emission sources.

4.3 Elemental Concentrations of Emissions

The heavy metal concentrations in the emissions for the different burning simulations are presented in Fig. 3 (accompanying values in Table S1). Presented in this table are the elements that have acceptable recovery using the method reported by Rosales and Lamorena-Lim (2015). Of all the elements detected, Pb appears to be in elevated concentrations, especially for MCC. It is not certain what the Pb source is, although its presence in unequal amounts in MCC and CCP, both of which used charcoal, may suggest that it came from the ingredients or the preparation of the chicken used for simulations rather than the charcoal itself. *p*-values (compared against MCC mean of 15 ± 11 Pb-μg m⁻³, latter is standard deviation) are 3, 5, 4, and 4 × 10⁻⁵ for CCP, KKP, MFP, and MKP respectively, and thus Pb can be said to have come from the substrate cooked (i.e., chicken or its seasonings).

Of the four fuel types, fuelwood (MFP) has the highest elemental emissions of Mn, Co, and Ni. On the other hand, Cu and As are highest from the sawdust (KKP). Sr is highest in CCP and Cd is almost the same for all four types, but slightly higher in CCP and MKP. For all samples, Ni and Cu are seen in notable concentrations. Co is also observed in all samples except MCC.

These differences in concentrations may be explained by the differences in fuel sources. The original environment of the different trees where the sawdust, charcoal, and fuelwood came from might have been subjected to surroundings exposed to metal contamination. However, as

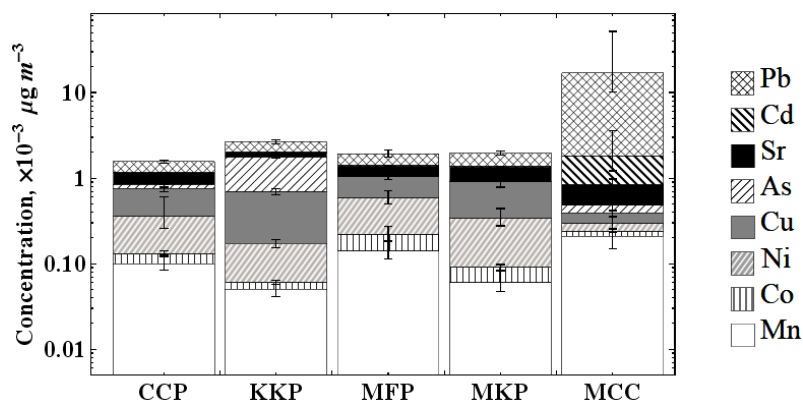
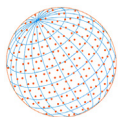


Fig. 3. Concentrations of selected elements that were reported to have acceptable recovery (see the “Methods” section). Concentrations are shown in a logarithmic scale, illustrating the vast range of elemental concentrations in different household fuel and cooking samples. Uncertainties shown stand for standard errors for each element detected in each fuel type.

most of the fuels are from organic materials, heavy metals are not expected to be dominant in the emissions.

4.4 Elemental Emission Factors

Tables 4 and 5 present elemental emission factors for MCC and four different fuel types. Table 4 shows the emission factors in terms of time, while Table 5 shows the emission factors in terms of the amount of fuel used. These values allow for the use of emission factors either when the activity data is the duration of time or the amount of fuel used. However, it should be noted that some of the values, such as emission factors for Pb and Cd (in ng kg-fuel⁻¹) have very high standard deviations and thus might not be appropriate factors to use for estimations. Moreover, the emission factors listed herein are most appropriate for the types of fuel closest to the ones tested in the burning emissions.

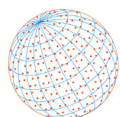
Table 4. Elemental emission factors (in ng min⁻¹) for different fuel types. Uncertainties shown are standard deviations.

Element	CCP	KKP	MFP	MKP	MCC
Mn	0.49 ± 0.28	0.25 ± 0.16	0.71 ± 0.51	0.32 ± 0.23	1.03 ± 1.24
Co	0.32 ± 0.22	0.16 ± 0.19	0.85 ± 1.69	0.19 ± 0.12	0.47 ± 0.37
Ni	1.16 ± 1.92	0.56 ± 0.24	1.87 ± 1.43	1.25 ± 1.12	0.32 ± 0.44
Cu	2.02 ± 1.06	2.72 ± 0.76	2.23 ± 1.18	2.87 ± 2.21	0.46 ± 0.35
As	0.43 ± 1.11	5.51 ± 1.08	0.06 ± 0.05	0.03 ± 0.01	0.46 ± 0.96
Sr	1.51 ± 0.39	1.08 ± 0.35	1.61 ± 0.73	2.02 ± 0.32	1.77 ± 1.77
Cd	0.12 ± 0.04	0.10 ± 0.04	0.16 ± 0.13	0.21 ± 0.27	4.96 ± 12.82
Pb	1.96 ± 1.04	3.55 ± 1.92	2.67 ± 2.77	3.01 ± 1.70	76.02 ± 151.42

Table 5. Elemental emission factors (in ng kg-fuel⁻¹)* for different fuel types. Uncertainties shown are standard deviations.

Element	CCP	KKP	MFP	MKP	MCC
Mn	54.48 ± 28.68	19.95 ± 12.42	557.99 ± 1183.76	98.58 ± 84.17	90.46 ± 105.35
Co	16.52 ± 12.88	5.11 ± 5.92	271.85 ± 552.04	36.69 ± 20.60	14.14 ± 13.96
Ni	134.73 ± 237.83	42.06 ± 18.14	1566.50 ± 2309.53	304.21 ± 309.14	22.71 ± 28.88
Cu	197.86 ± 76.43	196.61 ± 53.03	1839.49 ± 2831.49	737.81 ± 477.82	41.21 ± 29.81
As	52.32 ± 137.08	401.55 ± 63.43	23.56 ± 29.98	9.29 ± 3.23	34.95 ± 64.26
Sr	171.29 ± 33.95	79.95 ± 24.78	1274.40 ± 2058.24	566.04 ± 260.11	166.05 ± 159.97
Cd	13.93 ± 5.17	6.68 ± 3.22	146.91 ± 312.15	50.32 ± 47.51	373.19 ± 956.99
Pb	228.87 ± 134.14	246.30 ± 141.84	1442.99 ± 1951.58	852.03 ± 555.34	5629.43 ± 11,290.74

* per L fuel for kerosene.



Differences in the orders of magnitudes of the emission factors in Tables 4 and 5 are evident. Furthermore, MFP shows the greatest emissions per kg-fuel, meaning even a small amount of fuelwood can bring about large amounts of emissions. MKP also shows large amounts of emissions per amount of fuel used. This may be brought about by contaminants during the processing of the crude oil used for kerosene, and since this kerosene is sourced from a gasoline station, pollutants from mobile sources may have also been incorporated in this type of fuel. On the other hand, charcoal and sawdust—both plant derivatives—show lesser emissions per kg-fuel burned. Contaminants may have possibly been removed by previous drying or ashing processes that these materials have undergone prior to burning.

4.5 Water-soluble Ionic Species

The measured ion concentrations of all PM_{2.5} samples collected from the five tested materials are shown in Fig. 4 (accompanying values in Table S2). For MCC, CCP, KKP, and MFP, K⁺ and Cl⁻ have the highest concentrations among all the ions measured, while for MKP, Na⁺ was present in exceedingly high amount compared to the other ions. This may be indicative of Na⁺ bound to organics in kerosene. Total ionic concentration for MFP was the lowest among all fuels, while MKP and CCP show the highest total ion concentration.

Pearson correlation coefficients for the measured ions are shown in Table S6. MCC, CCP, KKP, and MFP all have high correlations for the ion pair K⁺ and Cl⁻, which is characteristic of particulate emissions from vegetation burning (Li *et al.*, 2003; Johnson *et al.*, 2006). Potassium, usually present in the ionic form in the aqueous phase, is important in the enzyme activity of plants. Moreover, electrochemical potential over the plasma membranes of plants are balanced by the transport of K⁺ and Cl⁻ (Westberg, 2003). In addition, the significant correlation between K⁺ and SO₄²⁻ for MCC is also attributable to biomass burning. As particles age, KCl particles are converted to K₂SO₄ and KNO₃ (Li *et al.*, 2003). Considering that *lechon manok* used charcoal, which is prepared by pyrolysis, some KCl particles initially present may have aged and converted to K₂SO₄ through time. However, since there is a lack of significant correlation between K⁺ and SO₄²⁻ for charcoal (CCP), this may also suggest that K₂SO₄ is produced during burning of the charcoal itself. For MCC, burning was slightly longer (1 hour and 20 minutes) than for charcoal (1 hour). In addition, the presence of the chicken may have contributed to the conversion process of the potassium salts.

Another notable correlation is that for Na⁺ and NO₃⁻ found uniquely in the MCC sample. This correlation was not found in CCP, and thus is not a charcoal-related marker, but may be characteristic of the chicken or its ingredients.

Significant correlations also exist between Na⁺ and SO₄²⁻ (0.96) and Na⁺ and Cl⁻ (0.70) in MKP. This may be indicative of organic salts as possible kerosene additives. Similarly, a correlation was found for Na⁺ and SO₄²⁻ (0.75) and Na⁺ and NH₄⁺ (0.77) in KKP, for which a little bit of kerosene was used to start the burning process. One possible source of these ions are antistatic additives, such as salts of organic acids and quaternary ammonium salts, that are used to increase the electrical conductivity of hydrocarbons such as gasoline and kerosene (Wauquier, 1995).

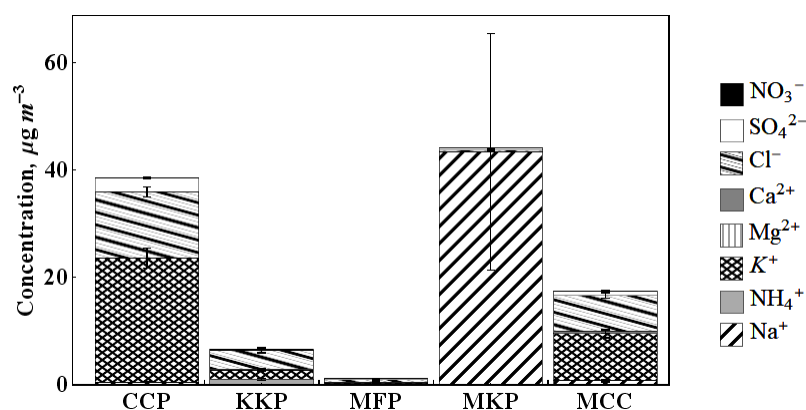
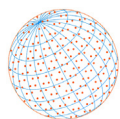


Fig. 4. Average measured ion concentrations for different fuel types tested. Negative concentrations are not reported.



For MFP, various ion pairs (other than K^+ and Cl^-) such as Mg^{2+} and SO_4^{2-} (0.71), Ca^{2+} and Cl^- (0.89), Ca^{2+} and SO_4^{2-} (0.67), and Ca^{2+} and NO_3^- were found. In addition to the fuel type itself, these ion pairs could be attributed to the chicken itself or the ingredients used to flavor the chicken.

4.6 Water-soluble Organic Carbon

Aside from the ionic composition, organic carbon is one of the major components of water-soluble components of atmospheric aerosols (Ram and Sarin, 2010; Sannigrahi *et al.*, 2006). Fig. 5 and Table S3 show the average WSOC ranging from 0.05 to $21.75 \mu\text{g C m}^{-3}$ for all the fuels sampled, the highest of which was KKP and lowest from MFP. While kerosene is made of hydrocarbons, it should be noted that these are long-chain (aliphatic) and cyclic hydrocarbons (Encyclopedia Britannica, 2016) and an incomplete combustion may result in water-insoluble organic compounds.

It can be noted that for biomass, the order of WSOC follows that of the particulate emission factors (i.e., $MFP < CCP < KKP$). MFP is also consistently low in water-soluble components (Figs. 4 and 5). In addition, while charcoal, sawdust, and fuelwood are all derived from biomass, it is interesting to note that the WSOC range of these fuels span two orders of magnitude. This range, as well as the order, may be attributed to differences not only in chemical makeup but also from the physical form (size)—sawdust was very fine, while charcoal and fuelwood were both bigger pieces and thus had less surface area, making its composition less accessible. Burning very fine sawdust, which had the greatest surface area, led to more efficient burning and possibly more complete combustion compared to the other two biomass fuels. Degradation via combustion of biomass components such as lignin, a major component of vegetation, gives rise to phenolic, ketonic and aldehydic functional groups in the WSOC (Sannigrahi, 2006). However, information on the speciation of the organic portion is sparse and can only be inferred indirectly from WSOC analyses.

4.7 Monosaccharide Anhydrides (Anhydrosugars) as Molecular Markers for Biomass Burning

Biomass burning emissions may be detected in atmospheric PM using levoglucosan and other related monosaccharide anhydrides (mannosan and galactosan) derived from the breakdown (dehydration) of cellulose, a major component of wood (Simoneit *et al.*, 1999). As such, these sugars are used as molecular markers for combustion of vegetation (Kuo *et al.*, 2008). In addition, these sugars, when correlated to K^+ , can be used as tracers for biomass burning (Jung *et al.*, 2014). The levels of monosugars detected in each fuel type is shown in Fig. 6 and Table S3. Total sugar levels are shown to be highest for KKP and MCC; on the other hand, CCP, MFP, and MKP are shown to have very low sugar levels compared to the former two. For elevated levels in KKP, this may be a function of the effective surface area of the fuel burned during cooking. Finer pieces of

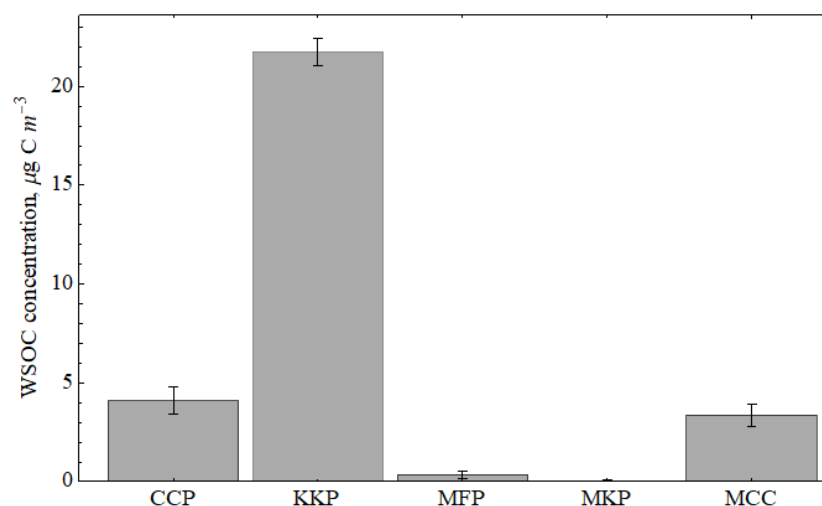


Fig. 5. Average measured WSOC for the different fuel types tested.

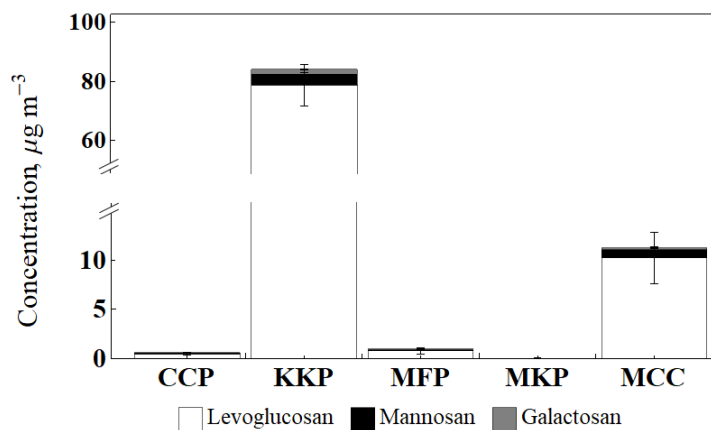
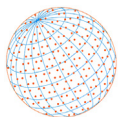


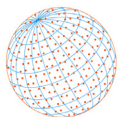
Fig. 6. Monosugars detected in fuel samples. Monosugars were detected less than $1 \mu\text{g m}^{-3}$ for MKP.

kusot in KKP allowed for more efficient breakdown of cellulose to its degradation products, and thus all three (levoglucosan, mannosan, and galactosan) are shown in abundance relative to the other fuel sample types. Sugars are not found in combustion products of fossil fuels such as kerosene (MKP), as shown in Fig. 6. While charcoal is biomass, it falls below the analytical window of levoglucosan test, for which the atomic H/C ratio only spans 0.8–1.6 (Kuo *et al.*, 2008). Since charcoal has already undergone pyrolysis during its preparation, it is expected that H/C ratio would be lower (i.e., most of it has been converted to black carbon or soot). As such, sugars were found in low levels in CCP. However, MCC, which also used charcoal, is shown to have about an order of magnitude total sugars compared to CCP. While these sugars may not come from the charcoal itself, they may have originated from the cooked substrate (i.e., chicken and spices stuffed inside such as lemongrass) instead.

To further explore the relationship between each sugar as well as with other ions, a correlation analysis was run (Tables S5 and S6). No significant correlations were observed for CCP. As for MKP, which is not biomass, levoglucosan and galactosan were not detected in any of the samples, and mannosan was detected in only three samples. Levoglucosan is highly correlated with mannosan, with Pearson coefficients ranging from 0.96–0.99 for MCC, KKP, and MFP. Levoglucosan is also highly correlated with galactosan for the fresher wood samples (sawdust and fuelwood), but correlation is lower between the two for MCC. Similarly, galactosan and mannosan are highly correlated for KKP and MFP but has a lower correlation coefficient for MCC. Nevertheless, these values confirm that the emission of these three sugars are related to burning vegetation. However, mannosan and galactosan were not found in samples of charcoal tested. Moreover, for the CCP PM samples where the sugars were found, correlation was not statistically significant. Since charcoal is burned wood, cellulose has already been broken down prior to use in cooking. However, for the MCC samples, the chicken was stuffed with lemongrass. The burning of the lemongrass leaves produced fresh cellulose breakdown products. Of all the samples, sawdust emitted the highest concentrations of all sugars. Since it was introduced as fine wood shavings, more wood is burned per unit time as compared to big chunks of fuelwood.

The potassium cation (K^+) has been previously reported in literature as a conventional biomass burning tracer (Mochida *et al.*, 2010) and a major constituent of biomass ash (Schmidl *et al.*, 2008). It has also been found to be moderately correlated with levoglucosan, mannosan, and galactosan (Jung *et al.*, 2014) in biomass. However, it may not exclusively come from biomass burning—for example, sea salt is another source of K^+ (Mkoma *et al.*, 2013). Thus, its ratio with any of the anhydrosugars (levoglucosan, mannosan, or galactosan) that are known to be biomass burning tracers themselves, e.g., Levo/K^+ , is an effective tool as a biomass burning tracer and can be used with confidence (Jung *et al.*, 2014).

The ratio of levoglucosan to mannosan (Levo/Man) has been used in the past as an indicator for specific types of biomass burnt (Schmidl *et al.*, 2011; Jung *et al.*, 2014), i.e., it has been proposed by Schmidl *et al.* (2008) as a tool to differentiate between hard- and softwood smoke. High ratios (ca. 14–15) are usually observed for hardwood, while low ratios (ca. 3.6–3.9) are

**Table 6.** Average levoglucosan to mannosan (Levo/Man) and levoglucosan to potassium (Levo/K⁺) ratios for different biomass burned.

	Levo/Man	Levo/K ⁺
MCC	13.14 ± 3.86	1.36 ± 1.16
KKP	21.27 ± 0.83	50.17 ± 13.82
MFP	7.06 ± 4.62	3.09 ± 4.87

usually observed for softwood (Schmidl *et al.*, 2008). Table 6 shows the average ratios obtained. Levo/Man ratios show a very small standard deviation for KKP, which means that levoglucosan and mannosan are emitted in proportional amounts during combustion and may thus be used as a tracer for red lauan sawdust/wood shavings. As for chicken and fuelwood burning, the Levo/Man ratio also presents a potential marker. However, the value obtained for the chicken grilling may be misleading because the value obtained in this study considers the presence of the lemongrass stuffing. Moreover, since there are many types of fuelwood that may be used for household cooking, having a range of Levo/Man ratios that is inclusive of more wood types will be beneficial as chemical fingerprint of biomass burning. On the other hand, a K⁺-sugar correlation was not existent in any of the samples in this study. It might be that the relationship is not linear, due to differences in the time it requires for K⁺ and the sugars to settle on the PM emitted. The lack of correlation may also be due to the specificity of the abundance of K⁺ from certain biomass types. Moreover, Levo/K⁺ ratios show large standard deviations for the ratios calculated herein; thus, this ratio may not be consistent throughout the burning of the fuel and may not be the best choice as a marker for the types of fuels sampled.

4.8 Overall Composition for Each Fuel Type

Fig. 7 shows the distribution of the total composition for each fuel type. For all fuel types, elemental composition was less than 1% of the total. Ion concentrations are shown in microequivalents per m³ (μeq m⁻³). Water-soluble components such as ions and organic carbon made up most of each fuel type's known composition, except for KKP, for which sugars made up about 75% of the known composition, thus showing that sugars can be a marker for these indigenous types of biomass. This is further supported by the presence of the ion pair K⁺-Cl⁻ which is also a known vegetation biomarker. On the contrary, samples that used processed fuel (CCP and MKP, both of which used the simple pan test) show that sugars make up less than 2% of the total determinable composition of the particulate. On the other hand, CCP and MCC, both charcoal-based, show a huge difference in the amount of sugars determined in each. Testing the MCC sample mean against the CCP mean (0.6 ± 0.4, latter is standard deviation) gives $p \approx 0$ (test statistic = 119.147). Thus, these two are significantly different, and the difference can be attributed to the sample substrate, i.e., chicken for MCC.

5 CONCLUSIONS

By employing a UPDDTS to sample different cooking systems in the Philippines, we have obtained some of the first measurements and chemical analyses of localized emissions—specifically, those generated by cooking with commonly used household fuels (charcoal, kerosene, sawdust, and fuelwood) and grilling chicken in the style of commercial rotisseries (*lechon manok*)—that affect developing Asian cities. We assessed the performance of the UPDDTS by evaluating the sampling conditions it provided, *viz.*, the wind velocity, *Re*, and emission rate.

Furthermore, we calculated emission factors for the PM and elements based on the measured mass concentrations, thereby demonstrating an inexpensive method for improving governmental emission inventories and the consequent policy making. The concentrations of the major PM-bound ions and sugars (levoglucosan, mannosan, and galactosan) confirmed the feasibility of using correlations between two ions, such as K⁺ and Cl⁻, and the ratio of levoglucosan to mannosan as chemical fingerprints of biomass burning in local urban areas, including indoor environments. Additionally, certain ionic pairs potentially indicated the presence of specific additives in a processed fuel or particular ingredients in a dish, whereas the WSOC content

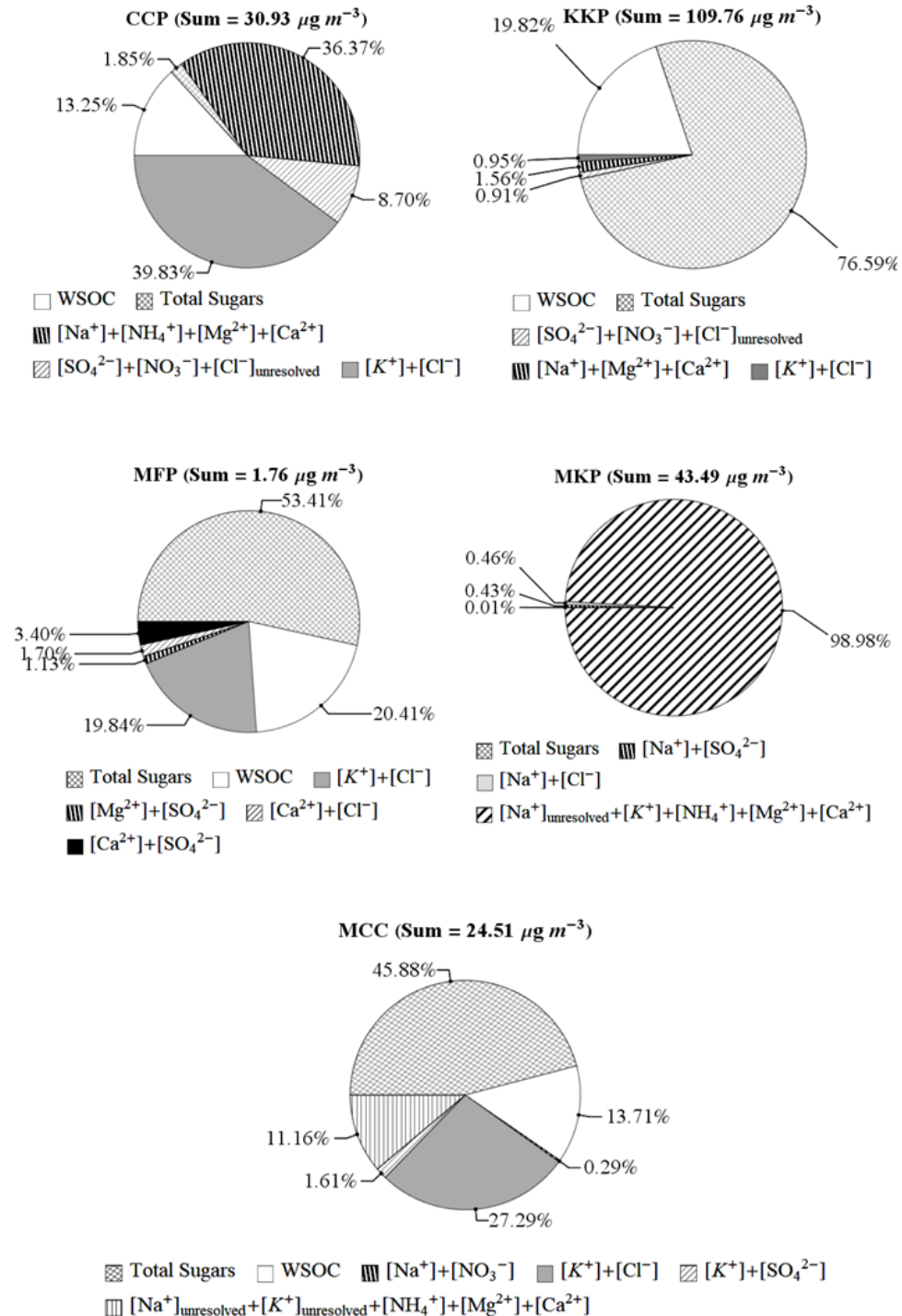
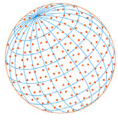
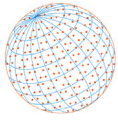


Fig. 7. Distribution of all compositions of each fuel type and sample. Water-soluble ions make up the most of MKP and CCP, while sugars make up the most of KKP, MFP, and MCC. WSOC is abundant in all samples except MFP. For figure clarity, any concentration $\leq 0.001 \mu\text{g m}^{-3}$ is not shown.

revealed a relationship between the surface area of a biomass fuel and the gas-to-particle-phase transformation of water-soluble organic combustion products, the latter of which creates a pathway for various pollutants into the human respiratory system.

We found lower PM emission factors for charcoal combustion but higher ones for kerosene combustion than those in the literature; hence, contributions from the latter fuel may be underestimated when the emission factors are drawn using previous references. We also



discovered that owing to the industrial processing of the charcoal and kerosene, which decreased their H/C ratios, these two fuels varied from the “fresher” (unprocessed) fuelwood and *kusot* in terms of the generated sugar content. However, when attributing the sugar composition to the fuel type, the cooking ingredients, as another factor, must be considered.

Finally, our recommendations for future studies include (1) testing additional materials that are specific to a local or regional setting, (2) chemically characterizing the particle-phase water-soluble organic carbon to better evaluate the gas–particle partitioning and particle growth, and (3) estimating the dose rates for different demographics.

ACKNOWLEDGMENTS

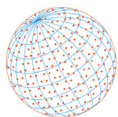
The authors are grateful to the following for the funding granted for this study: Clean Air Asia and International Environmental Research Center in 2014–2016 and GIST Research Institute (GRI) grant funded by the Gwangju Institute of Science and Technology (GIST) in 2019–2021. The UPDDTS was installed by Fernando Llano, Jr. Illustrations and dimensions were provided by Daryl Marc On and Ivan Genelsa, and the calculation of Reynolds number by Artemio Innocencio E. Pascual. Wind tunnel experiments were performed with the assistance of Paola Angela Bañaga, Gabrielle Aleksa Castillo, Phillip Joshua Bernadas, and Anton Rodriguez. Ion chromatography analysis was done by Enrique Mikhail Cosep at Korea Research Institute of Standards and Science (KRISS).

SUPPLEMENTARY MATERIAL

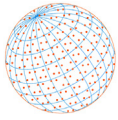
Supplementary data associated with this article can be found in the online version at <https://doi.org/10.4209/aaqr.200581>

REFERENCES

- Aguilar, B.J.E., Apal, Z.H., De Jesus, R.B., Erni, M.E., Lipardo, K.A., Rafael, J.B.M., Sese, L.V., Dela Cruz, M.H.T. (2017). Effectiveness of a fuel-efficient cookstove in the reduction of perceived respiratory symptoms among mothers in selected households of purok 6 in brgy santa cruz, sto tomas, Batangas: A quasi-experimental study. *Respir. Med.* 132, 277. <https://doi.org/10.1016/j.rmed.2017.07.046>
- Baldauf, R.W., Devlin, R.B., Gehr, P., Giannelli, R., Hassett-Sipple, B., Jung, H., Martini, G., McDonald, J., Sacks, J.D., Walker, K. (2016). Ultrafine particle metrics and research considerations: Review of the 2015 UFP workshop. *Int. J. Env. Res. Pub. He.* 13, 1054. <https://doi.org/10.3390/ijerph13111054>
- Clean Cooking Alliance (CCA) (2018). Harmonized laboratory test protocols. <https://www.cleancookingalliance.org/technology-and-fuels/testing/protocols.html>
- Deutsche Gesellschaft für Internationale Zusammenarbeit (GIZ) (2012). Emission inventory of major air pollutants in Iloilo city. Clean Air for Smaller Cities in the ASEAN region (CASC).
- Dhampapala, R. Claiborn, C. Jimenez, J., Corkill, J., Gullett, B., Simpson, C., Paulsen, M. (2007). Emission factors of PAHs, methoxyphenols, levoglucosan, elemental carbon and organic carbon from simulated wheat and Kentucky bluegrass stubble burns. *Atmos. Environ.* 41, 2660–2669. <https://doi.org/10.1016/j.atmosenv.2006.11.023>
- Encyclopedia Britannica (2016). Kerosene – chemical compound. The Editors of Encyclopaedia Britannica. <https://www.britannica.com/science/kerosene> (accessed 18 April 2020).
- Engineering ToolBox (2003). Reynolds Number. https://www.engineeringtoolbox.com/reynolds-number-d_237.html (accessed 12 January 2021).
- European Environment Agency (EEA) (2009). EMEP/Corinair Emissions Inventory Guidebook. Technical Report No.9/2009.
- Gloor, R. (2014). Air pollution and health. BusinessWorld Online. <http://www.bworldonline.com/content.php?section=Weekender&title=air-pollution-and-health-&id=85329>.
- Hildemann, L.M., Cass, G.R., Markowski, G.R. (1989). A dilution stack sampler for collection of



- organic aerosol emissions: Design, characterization and field tests. *Aerosol Sci. Tech.* 10, 193–204. <https://doi.org/10.1080/02786828908959234>
- Jenkins, B.M. (1990). Development of test procedures to determine the emissions from open burning of agricultural and forestry wastes. California Air Resource Board.
- Johansson, C., Norman, M., Burman, L. (2009). Road traffic emission factors for heavy metals. *Atmos. Environ.* 43, 4681–4688. <https://doi.org/10.1016/j.atmosenv.2008.10.024>
- Johnson, K. S., de Foy, B., Zuberi, B., Molina, L. T., Molina, M. J., Xie, Y., Laskin, A., Shutthanandan, V. (2006). Aerosol composition and source apportionment in the Mexico City Metropolitan Area with PIXE/PESA/STIM and multivariate analysis. *Atmos. Chem. Phys.* 6, 4591–4600. <https://doi.org/10.5194/acp-6-4591-2006>
- Jung, J., Lee, S., Kim, H., Kim, D., Lee, H., Oh, S. (2014). Quantitative determination of the biomass-burning contribution to atmospheric carbonaceous aerosols in Daejeon, Korea, during the rice-harvest period. *Atmos. Environ.* 89, 642–650. <https://doi.org/10.1016/j.atmosenv.2014.03.010>
- Kulkarni, P. Chellam, S., Flanagan, J.B., Jayanty, R.K.M. (2007). Microwave Digestion—ICP—MS for elemental analysis in ambient airborne fine particulate matter: Rare earth elements and validation using a filter borne fine particle certified reference material. *Anal. Chim. Acta* 599, 170–176. <https://doi.org/10.1016/j.aca.2007.08.014>
- Kuo, L.J., Herbert, B.E., Louchouart, P. (2008). Can levoglucosan be used to characterize and quantify char/charcoal black carbon in environmental media? *Org. Geochem.* 39, 1466–1478. <https://doi.org/10.1016/j.orggeochem.2008.04.026>
- Li, J. Posfai, M., Hobbs, P.V., Buseck, P.R. (2003). Individual aerosol particles from biomass burning in southern Africa: 2. Compositions and aging of inorganic particles. *J. Geophys. Res.* 108, 8484. <https://doi.org/10.1029/2002JD002310>
- Mkoma, S.L., Kawamura, K., Fu, P.Q. (2013). Contributions of biomass/biofuel burning to organic aerosols and particulate matter in Tanzania, East Africa, based on analyses of ionic species, organic and elemental carbon, levoglucosan and mannosan. *Atmos. Chem. Phys.* 13, 10325–10338. <https://doi.org/10.5194/acp-13-10325-2013>
- Mochida, M., Kawamura, K., Fu, P., Takemura, T. (2010). Seasonal variation of levoglucosan in aerosols over the western North Pacific and its assessment as a biomass-burning tracer. *Atmos. Environ.* 44, 3511–3518. <https://doi.org/10.1016/j.atmosenv.2010.06.017>
- Philippine Statistical Authority (PSA) (2014). Census of Population and Housing (CPH) 2010. <https://psa.gov.ph/statistics/census/population-and-housing/2010-CPH>
- Philippine Statistical Authority (PSA) (2016). Highlights of the Philippine population 2015 census of population. <https://psa.gov.ph/content/highlights-philippine-population-2015-census-population>
- Ram, K., Sarin, M.M. (2010). Spatio-temporal variability in atmospheric abundances of EC, OC and WSOC over Northern India. *J. Aerosol Sci.* 41, 88–98. <https://doi.org/10.1016/j.jaerosci.2009.11.004>
- Rosales, C.M.F., Lamorena-Lim, R.B. (2015). Possible speciation of heavy metals in indoor air particulate matter near a landfill area. 3rd Annual International Conference on Chemistry, Chemical Engineering and Chemical Process (CCECP 2015) Conference Proceedings. pp. 87–91. https://doi.org/10.5176/2301-3761_CCECP15.19
- Saksena, S., Subida, R., Büttner, L., Ahmed, L. (2007). Indoor air pollution in coastal houses of southern Philippines. *Indoor Built Environ.* 16, 159–168. <https://doi.org/10.1177/1420326X07076783>
- Sannigrahi, P., Sullivan, A.P., Weber, R.J., Ingall, E.D. (2006). Characterization of water-soluble organic carbon in urban atmospheric aerosols using solid-state ¹³C NMR spectroscopy. *Environ. Sci. Technol.* 40, 666–672. <https://doi.org/10.1021/es051150i>
- Schmidl, C., Luisser, M., Padouvas, E., Lasselsberger, L., Rzaca, M., Ramirez-Santa Cruz, C., Handler, M., Peng, G., Bauer, H., Puxbaum, H. (2011). Particulate and gaseous emissions from manually and automatically fired small scale combustion systems. *Atmos. Environ.* 45, 7443–7454. <https://doi.org/10.1016/j.atmosenv.2011.05.006>
- Simoneit, B.R.T., Schauer, J.J., Nolte, C.G., Oros, D.R. Elias, V.O., Fraser, M.P., Rogge, W.F., Cass, G.R. (1999). Levoglucosan, a tracer for cellulose in biomass burning and atmospheric particles. *Atmos. Environ.* 33, 173–182. [https://doi.org/10.1016/S1352-2310\(98\)00145-9](https://doi.org/10.1016/S1352-2310(98)00145-9)
- Suranaree University of Technology (SUT) (2012). Final Report: Emission Inventory of Major Air Pollutants in Nakhon Ratchasima Municipality (NRM). German International Cooperation (GIZ). pp. 44–45.



- United Nations (UN) (2018). Sustainable Development Goals: 7. Affordable and Clean Energy. <https://www.un.org/sustainabledevelopment/energy/> (accessed 15 December 15 2018)
- United States Environmental Protection Agency (U.S. EPA) (2009). AP-42: Compilation of Air Pollutant Emission.
- Wauquier, J.P. (1995). Petroleum Refining. Imprimerie Chirat, Saint-Just-la-Pendue.
- Westberg, H.M., Byström, M., Leckner, B. (2002). Distribution of potassium, chlorine, and sulfur between solid and vapor phases during combustion of wood chips and coal. *Energy Fuel* 17, 18–28. <https://doi.org/10.1021/ef020060l>
- Wilson, D., Rapp, V.H., Caube, J.J., Chen, S., Gadgil, A. (2017). Verifying mixing in dilution tunnels: How to ensure cookstove emissions samples are unbiased. Lawrence Berkeley National Laboratory, University of California. <https://escholarship.org/uc/item/5g19965j>
- World Health Organization (WHO) (2014). WHO indoor air quality guidelines: Household fuel combustion. <https://www.who.int/airpollution/guidelines/household-fuel-combustion/recommendation1/en/>
- World Health Organization (WHO) (2016). Global Health Observatory Data Repository.
- Yee, J. (2018). Charcoal use exacts heavy toll on public health, economy. *Philippine Daily Inquirer*. <https://newsinfo.inquirer.net/1057082/charcoal-use-exacts-heavy-toll-on-public-health-economy>